Supplementary Material

Supplementary Materials and Methods

ATPase activity was determined by measuring concentrations of released phosphate using a modified malachite green colorimetric assay (protocol kindly provided by Prof. Thomas Langer, Cologne, Germany) based on the ATPase assay described by Chan et al. (Chan *et al.*, 1986). A solution of 1 mM malachite green and 8.5 mM ammonium molybdate was supplemented with 0.1 % Triton X-100 shortly before use to yield the assay buffer. A reaction was composed of 47 µl MK0840 full-length protein solution (1 mg/ml), water (for determination of the natural hydrolysis of ATP) or KH_2PO_4 (for standard curve determination), respectively, 2 µl ATP-MgAc mix (50 mM ATP, 100 mM MgAc), 1 µl ZnAc-DTT mix (1.25 mM ZnAc, 25 mM DTT) and 800 µl assay buffer, incubated at 25°C for 1 min and supplemented with 100 µl of 34% citric acid. After an incubation for 40 min at 25°C product formation was determined at 640 nm. All measurements were set up in triplicates and standard deviations were calculated. Phosphate release (µM) was determined and plotted for ATP alone (in water) and for ATP supplemented with full-length MK0840 incubated at 25°C for 20 h.

Kinase activity was determined similar to the assay performed for *E. coli* L-rhamnulose kinase (Grueninger & Schulz, 2006). The reaction buffer contained 20 mM Tris/HCl pH 7.5, 200 mM NaCl, 5 mM $MgCl_2$, 75 mM KCl, 8 units/ml of L-lactate dehydrogenase (Sigma-Aldrich), 16 units/ml of pyruvate kinase (Sigma-Aldrich), 0.9 mM ATP, 0.9 mM phosphoenolpyruvate, 0.45 mM NADH, 10 mM glucose for the positive control yeast hexokinase (Sigma-Aldrich) assayed with 0.2 units/ml or 10 mM of 45 different carbohydrates (Supplementary Table S1) assayed with 50 µg/ml of full-length MK0840 and truncated MK0840 (L37-T358), respectively. The reaction was kept at 25°C and 42°C, respectively. The decrease of the NADH absorption was monitored every 5 minutes for 60 min at a wavelength of 366 nm.

Supplementary Table S1. Substances tested in kinase assay with MK0840

1,5-anhydro-D-mannitol	L(-)-fucose
2-deoxy-D-glucose	L(-)-sorbose
acetate	L(+)-arabinose
adonitol	L-threonine
butyrate	maltose
D(-)-erythrose	mannitol
D(-)-fructose	methyl-β-D-glucopyranoside
D(-)-ribose	methyl-β-D-mannopyranoside
D(-)-threose	N-acetyl-D-galactosamine
D(+)-galactose	N-acetyl-D-glucosamine
D(+)-lactose	N-acetyl-D-mannosamine
D(+)-mannose	N-acetylmuramic acid
D(+)-talose	octyl-β-D-glucoside
D(+)-trehalose	pantothenic acid
D(+)-xylose	polyethyleneglycol 200
dextrose	potassium-D-gluconate
D-glucosamine HCl	propionate
D-glucose	L-rhamnose
D-mannosamine HCl	succinate
isobutyrate	sucrose
ethylene glycol	thiamine
glycerol	xylite
E. coli polar lipids in 1% dodecylmaltoside	

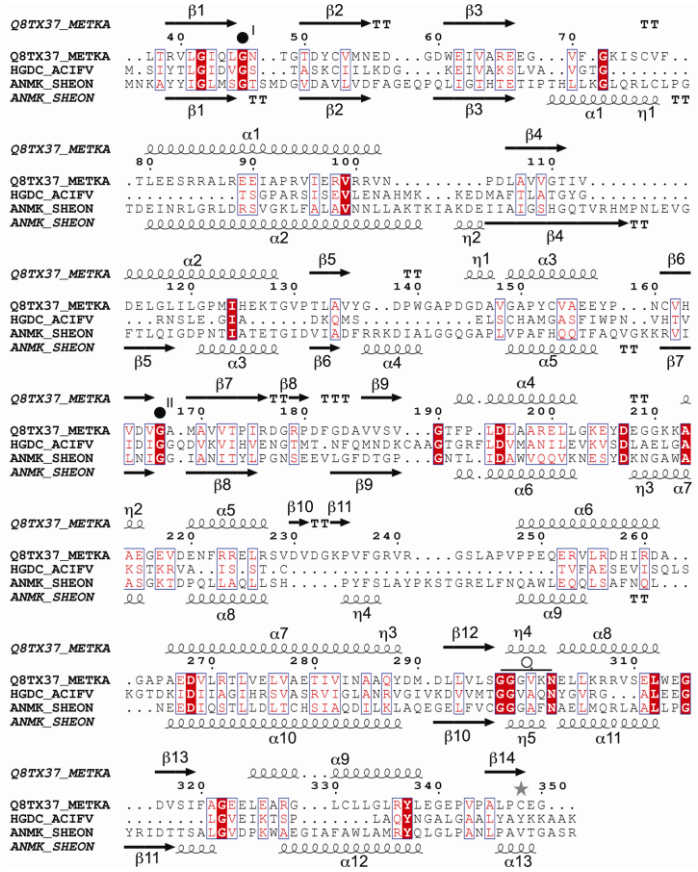

Supplementary Figure S1.

Structure based multiple sequence alignment of MK0840 (Q8TX37_METKA), HgdC from *A. fermentans* (HGDC_ACIFV, PDB ID 1HUX) and AnmK from *S. oneidensis* (ANMK_SHEON, PDB ID 3CQY). Proteins are labeled by UniProtKB identifiers. Highly conserved residues are printed in white on a red background. Residues with conservative substitutions are indicated with red letters. Secondary structure elements of MK0840 and *So*AnmK are also shown. 3_{10}-helices are indicated by η, β-turns by T and residues showing alternative conformations are marked with grey stars. The adenosine (ADENOSINE) and phosphate binding regions (PHOSPHATE I/II) are indicated by open and solid circles, respectively.

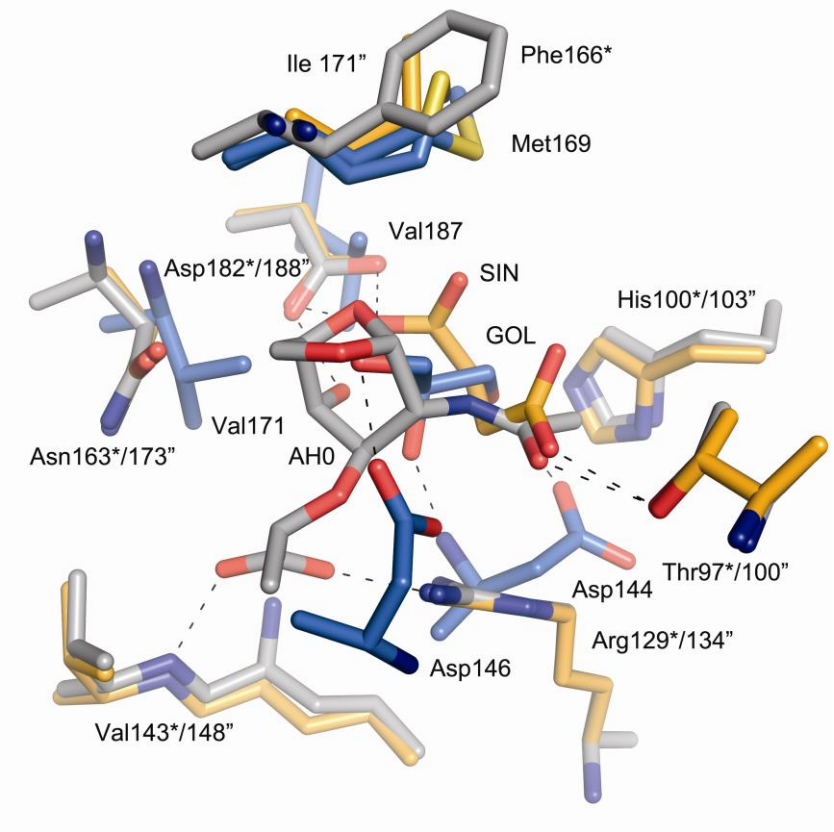

Supplementary Figure S2.

Comparison of substrate-binding and active site residues. Superimposition of the substrate-binding sites and bound ligands of *So*AnmK (orange), *Pa*AnmK (grey) and MK0840-ADP^{closed} (slate), which shows their distinct architecture. *So*AnmK residues are indicated by (“), and *Pa*AnmK by (*).

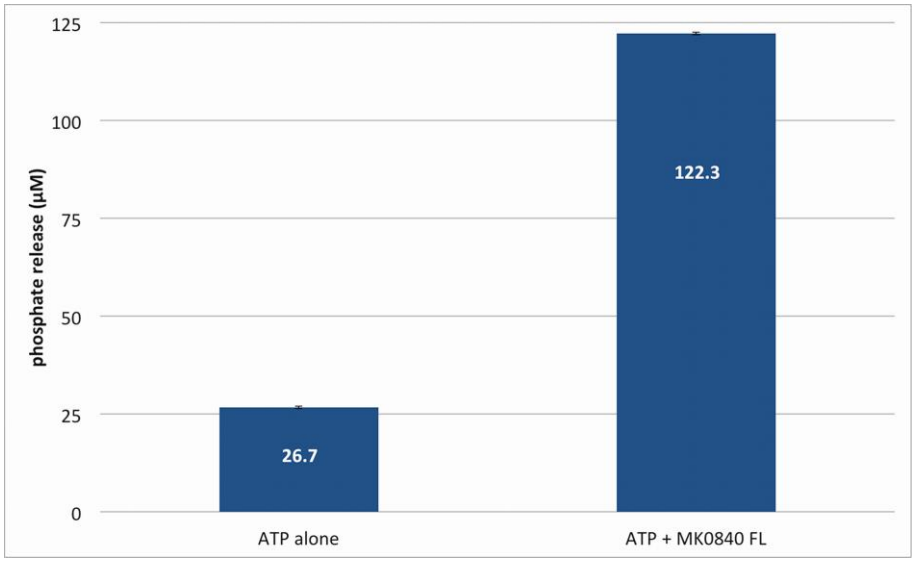

Supplementary Figure S3.

ATPase activity of MK0840 full-length protein. The release of inorganic phosphate from ATP was determined using a malachite green assay. A 5-fold increase in ATP hydrolysis in the presence of MK0840 full-length (ATP + MK0840 FL) was observed compared to background (ATP alone). The mean values from triplicate measurements and their standard deviation were plotted.

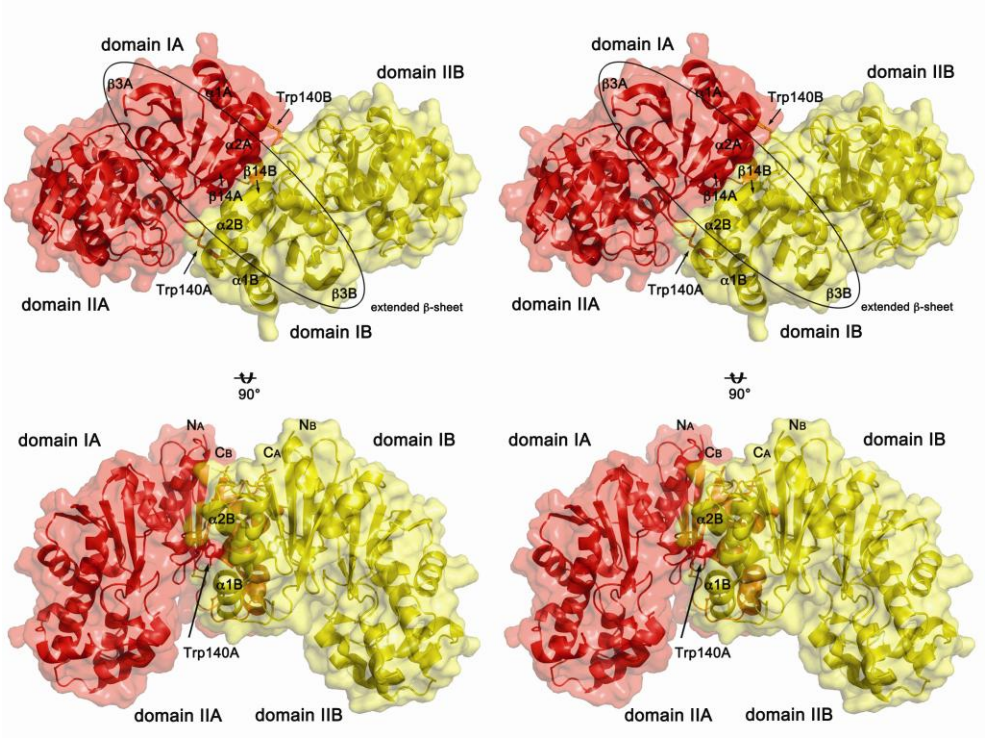

Supplementary Figure S4.

Stereo image of the top and side view of the MK0840 dimer. Both domains I build up an extended β-sheet. Protomers A and B are colored in red and yellow, respectively. The molecular surface and structural elements involved in dimer formation are also shown.

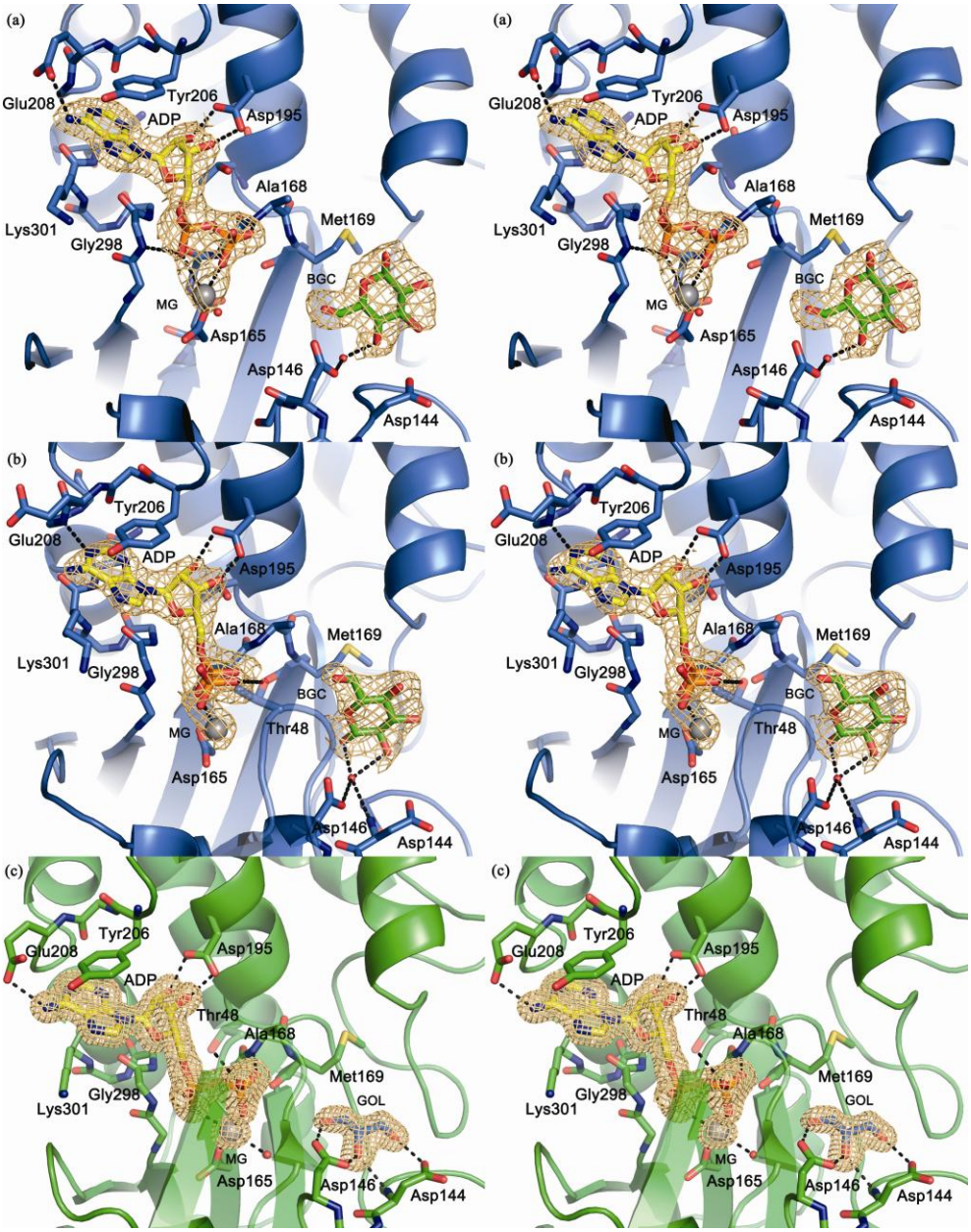

Supplementary Figure S5.

Stereo image of the nucleotide and substrate binding sites of the open and closed form of MK0840. (a) In protomers B and D of MK0840-ADP^{open} the β-phosphate of ADP points towards the β-D-glucose (BGC) molecule and (b) in protomers A and C towards Thr48. Also the set of residues coordinating the adenine and ribose moiety differ. In protomers A and C (b) interactions with Ala168 and Glu208 are missing but a new interaction with Thr48 is

formed. (c) In MK0840-ADP^{closed} glycerol (GOL) is bound. The ADP molecule in (c) adopts the same conformation as in (a), but interacts simultaneously with Ala168 and Thr48, leading to domain closure. In all six protomers of both MK0840-ADP forms, the adenine moiety of ADP is stacked against the phenol ring of Tyr206 and the hydroxyl groups of the ribose are coordinated by Asp195. For better visibility, the loop containing Thr48 was removed in (a). In (a)-(c) $2F_o$-F_c OMIT electron density maps (light orange) of the ADP molecule, the Mg^{2+} ion, BCG (a) and (b) and GOL (c) contoured at 1.0σ are shown.